

Nanoscale Materials for Tackling Brain Cancer: Recent Progress and Outlook

Elena A. Rozhkova

This article reports on recent progress in the development of advanced nanoscale photoreactive, magnetic and multifunctional materials applicable to brain cancer diagnostics, imaging, and therapy, with an emphasis on the latest contributions and the novelty of the approach, along with the most promising emergent trends.

1. Introduction

The molecular design of functional materials at nanoscale supports innovation expected to revolutionize present technology and overcome societal challenges including sustainable energy supply, information storage, and the advancement of medical treatments for fatal diseases such as cancer. In the cancer context, nanotechnology will lead to a new generation of diagnostic and therapeutic technologies, creating dramatically increased outcomes and improving the quality of life for millions. Recently, the National Institutes of Health (NIH) identified four main types of cancer characterized by the lowest survival rates as targets for new nanotechnology discoveries—brain, lung, ovarian and pancreatic cancers.^[1] This article reports upon recent progress in the development of advanced nanoscale functional materials applicable to brain cancer diagnostics, imaging, and therapy, with an emphasis upon the latest contributions and the novelty of the approach, along with the most promising emergent trends.

While the central focus of this review is the development of advanced nanoscale materials, in order to better understand strategies for design and application of nanoplatforms a brief introduction to brain cancer, including its characteristics, specific nature, prognosis, and major challenges associated with its diagnostics and treatment, is included in Section 2.

Diverse nanoengineered materials and devices demonstrate great potential to interface with the central nervous system (CNS).^[2] This report focuses mostly on two classes of materials prospective in interfacing with CNS cancers. These materials are intrinsically responsive to the application of external stimuli, such as light or magnetic field. A third class hybrids include both optical and magnetic components. Section 3 summarizes the most recent advances in brain

cancer therapy and imaging based upon photo-responsive nanoscale materials. The application of organic dye photosensitizers to light-based advanced medical technologies, known as Photodynamic Therapy (PDT), has a long and successful history in intraoperative imaging and adjuvant therapy for brain cancer. With the development of modern nanoplat-

forms, it has become attractive to incorporate pigments into a variety of natural or synthetic polymeric nano-shells. This approach may lead to nearly endless possibilities for the synergistic combination of multiple modalities into one advanced hybrid nanomaterial for targeted drug delivery, multimodal imaging, and enhanced therapeutic efficacy. Another group of photo-responsive materials includes inorganic semiconductor colloid nanocrystals. Similar to PDTs based upon organic dyes, this approach also incorporates three principal components: light, oxygen, and a photoreactive material. The semiconductor photocatalyst particles absorb energy from light, which is in turn transferred to molecular oxygen, producing cytotoxic reactive oxygen species (ROS) harmful to cancerous cells. Unique tunable plasmonic and photothermal properties of gold colloids make these materials attractive both in imaging and tumor thermal ablation. Recent application of gold nanomaterials in brain imaging and thermal therapy is also summarized in Section 3.

The application of magnetic materials enables unprecedented functionality in the construction of nanohybrids and the development of powerful imaging techniques and therapy. In neurooncology, superparamagnetic nanoparticles are mainly utilized for magnetic resonance imaging (MRI) and magnetically induced hyperthermia. Section 4 discusses the successful demonstration of a platform based upon nanomagnetic materials to tackle brain cancer. The most remarkable progress to date (currently in stage II clinical trials) was achieved via magnetic hyperthermia or ablation of brain cancer using aminosilane-coated superparamagnetic magnetite nanoparticles.^[3a,d] Recently another novel magneto-mechanical approach for brain cancer destruction has been suggested.^[4] This strategy utilizes bio-functionalized ferromagnetic materials,^[4,5] or so-called soft magnets, with a spin-vortex ground state. In this material, cytostatic effects have been demonstrated using *ac* fields at unprecedentedly low frequencies (tens of Hz) through intervention into cellular signaling and calcium ionic homeostasis.

A third group includes multifunctional hybrids. Owing to the infinite possibilities afforded by nanoscale approaches to integrate multivalent functions in a single material, a variety of recent publications describe composite materials in which every

Dr. E. A. Rozhkova
Center for Nanoscale Materials
Argonne National Laboratory
9700 South Cass Avenue,
Argonne, IL 60439-4806, USA
E-mail: rozhkova@anl.gov

DOI: 10.1002/adma.201004714

component of a hybrid plays significant roles in biorecognition, targeting, multimodal imaging, and therapy. Combination of magnetic particles and quantum dots and biological molecules such as proteins, leader peptides and oligonucleotides (aptamers, siRNA) results in multivalent structures with synergistically enhanced properties suitable for brain cancer diagnostics and treatment. These multimodal hybrids are nominally classified as multifunctional materials and are presented in Section 5.

Natural anatomical (cranium) and physiological (i.e., the blood brain and blood tumor barriers, BBB and BTB, respectively) blockages represent obstacles which therapeutic tools must overcome. Engineered nanoplateforms offer unprecedented pathways to overcome or bypass these biological limits and deliver therapeutic agent directly to brain tumor. The great example of remarkable advancing of a great technological idea in the field of brain cancer therapy is combining of nanocarriers with boron neutron capture therapy (BNCT),^[6] which is one of the oldest adjuvant brain cancer therapies.^[7] While BNCT was proposed years ago^[8] as a promising method based upon the nuclear reaction of two essentially nontoxic species, non-radioactive boron ¹⁰B and low-energy thermal neutrons, this method has not become routine in clinical application, mostly because it is difficult to deliver high concentrations of ¹⁰B to brain tumor cells. The development of modern nanotechnology tools, especially for targeting and delivery, promises to address this difficulty. BNCT is only mentioned here in the context of tumor targeting and the convection-enhanced delivery method, and the reader is encouraged to get familiar with abovementioned articles.^[6] Section 6 is devoted to recent strategies for delivery and targeting of materials to the brain and application of external stimuli which are crucial for the success and efficacy of any medical technology directed to the CNS.

Finally, the conclusion Section 7 summarizes recent progress and surveys future trends in brain cancer diagnostics and therapy utilizing advanced materials.

2. Brain Cancer Outline: Prognosis, Biology and Special Features

Malignant glioblastoma and medulloblastoma represent nearly all of the common primary (de novo) CNS cancers of adult and pediatric populations, respectively.^[9] These brain tumors carry the most aggressive designations (grades III and IV) according to the World Health Organization (WHO) classification.^[10] For example, glioblastoma patients have a median survival time of less than 15 months after surgical intervention followed by radio- and chemotherapy.^[11,12] Failed therapy is most often associated with local reappearance of the tumor.^[13] Although radiation and chemotherapy have been more successful in combating childhood medulloblastoma, with 5-year survival rates now as high as 70–80%,^[14] the long-term side effects of these conventional therapies can be severe.

Most brain cancers are believed to abnormally derive from glial cells, neurons, or their less differentiated precursors, which via regular development should differentiate into mature functional cells—neurons, astrocytes, and oligodendrocytes^[9] (see **Figure 1**). Numerous molecular aberrations likely



Elena Rozhkova received her Ph.D. degree in Chemistry from the Lomonosov's Academy of Fine Chemical Technology (Moscow, Russia) in 1997. She has since worked as the JSPS postdoctoral fellow at the Institute of Multidisciplinary Research for Advanced Materials, Tohoku University (Sendai, Japan) and then as a Research Staff Member at the Department

of Chemistry, Princeton University (USA). Currently she is a Staff Scientist at the Center for Nanoscale Materials, Argonne National Laboratory, one of the US Department of Energy's Office of Science premier user centers for interdisciplinary research at the nanoscale. Her research interests include stimuli-responsive nano-bio composites, nanomaterials for energy and molecular signaling, synchrotron X-ray imaging of bioenergetic processes.

to be linked to brain cancer development were recently thoroughly reviewed.^[9] This review mentions only a portion of those which are relevant to recently developed strategies for the design of nanoplateforms targeted to brain cancer. For example, genetic abnormalities associated with brain cancerogenesis include mutations in tumor suppressor genes such as *TP53* and *RB*, which are responsible for regulation of apoptosis and

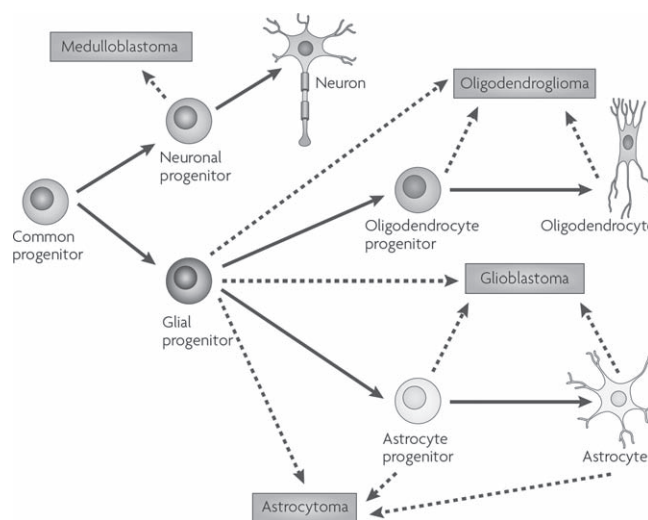


Figure 1. Brain tumors lineage tree. Common progenitors (ancestor cells) are thought to produce committed neuronal and glial progenitors that eventually differentiate into mature neurons, astrocytes and oligodendrocytes. Although the precise cells of origin for brain tumors remain largely unknown, a selection of likely candidates for each (dashed arrows) is indicated. Reproduced with permission.^[9] Copyright 2010, Nature Publishing Group.

control of angiogenesis (blood-vessel formation) in normal cells.^[9] As a result, defects in the natural molecular mechanisms of programmed cell death tremendously contribute to progression of the cancer and its resistance to conventional chemotherapy. Therefore, induction of cancer cells programmed death such as apoptosis is of great clinical significance. Another important target for novel therapies are genes expressing the epidermal growth receptor (EGFR) variant III deletion mutant (EGFR vIII), which has been identified in cancerous, but not in healthy, cells.^[9] Promising new technology uses hybrid materials capable of controlled delivery of small interfering RNA (siRNA) to silence this key pathway for brain cancer development and progression. Another relevant feature of brain cancer is its association with specifically altered immune pathways—for instance, the expression of a membrane receptor to interleukin 13 (IL13), which is a key signaling Th2 cytokine regulator for malignancy and inflammation.^[15a,d] As a matter of fact, the IL13 receptor (IL13R) is not expressed by healthy cells^[16a-c] and has been successfully employed for the targeting of cytotoxic elements, including toxins,^[16a] viruses,^[17] gold-silica immunonanospheres,^[18] TiO₂ semiconductor nanocrystals,^[19] and ferromagnetic microdisks,^[4] to brain cancer cells. Consequently, antibody-based immuno-targeting to specific receptors, such as IL13R and EGFRvIII, represents an important principle for the bottom-up construction of nanobio hybrid systems.

3. Photo-responsive Nanomaterials

While surgical intervention remains the most radical method of brain cancer treatment, photoactive materials can serve as important supporting tool. Their use for intraoperative imaging helps to avoid excessive excision of brain tissue responsible for intellectual and behavioral functions and reduces harm to patients quality of life. In addition, brain neoplasms tend to diffusively infiltrate healthy tissue; and a photocatalyst (even one not serving as a fluorescent marker; see examples below) can be used in adjuvant intraoperative light therapy to clear residual cancer cells and reduce the possibility of cancer reoccurrence. A comprehensive historical outline of light therapies based upon photoactive organic chemical compounds or photosensitizers (PS), which also describes the current progress of PDT for bioimaging, was recently given in an excellent review.^[20] The general scheme of “classical” PDT includes three principal components: PS or natural dye precursors (such as δ -aminolevulinic acid), light and oxygen. The absorption of light energy by the PS is followed by energy dissipation from the excited state via two major pathways: 1) the emission of fluorescence suitable for cancer detection, and 2) energy transfer to molecular triplet oxygen, producing reactive oxygen species (ROS) able to photooxidize bioorganic molecules and terminate cancer cells,

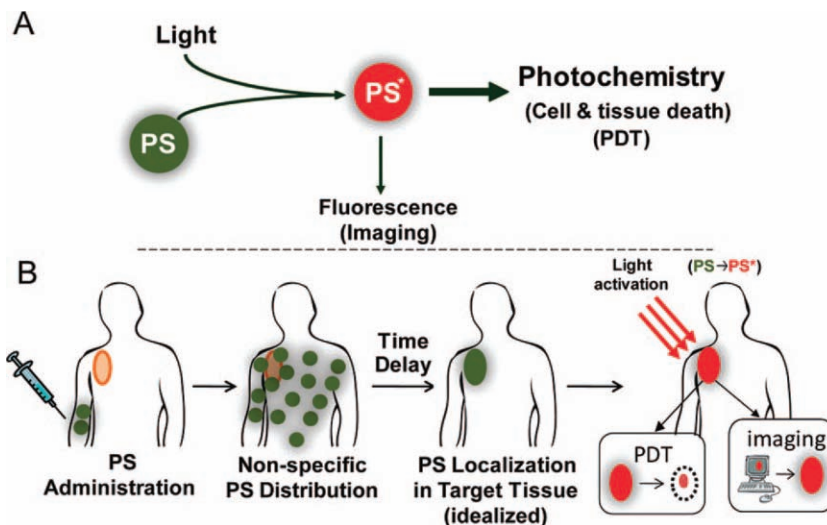


Figure 2. A) Schematic representation of PDT where PS is a photo-inducible multifunctional agent, which upon light activation can serve as both an imaging agent and a therapeutic agent. B) Administration, localization, and light activation of the PS for PDT or fluorescence imaging in vivo. Reproduced with permission.^[20] Copyright 2010, American Chemical Society.

Figure 2.^[20] This article focuses mainly on recent examples of the successful application of nanoscale photoactive materials, such as dye-loaded polymer supramolecular structures and semiconductor colloid nanocrystals, to brain cancer PDT. In addition, approaches utilizing other photonic hybrid materials, such as gold nanoparticles, were reported to be useful for Photothermal Ablation Therapy of brain cancer cells.^[18] In spite of the diversity of chemical composition, structure and mechanism of action, all PS approaches share one common requirement—they must be inducible in a spectral window near the optimal biological optical area. While the maximum transparency of the epidermis lies between 800–1100 nm, it has been demonstrated that glioblastoma tissue is susceptible to the application of 630 nm laser light via optical fiber with remarkable optical penetration depth of ~3.1 mm in the context of brain cancer PDT.^[21a-e]

3.1. Dye-loaded Polymer Nanoparticles

With the development of modern nanoplatforms, the incorporation of organic dye molecules into a variety of polymeric self-assembled nano-scaffolds became valuable technique. These systems cannot use dye precursors because, without direct contact with the biological system, a caged precursor cannot be enzymatically transformed into a “mature” PS. At the same time polymer matrices are believed to have a sufficient degree of porosity to allow an entrapped PS to react with molecular oxygen.^[22] The encapsulation of dyes into a polymeric matrix can reduce certain side effects of PDT. Moreover, this approach allows the introduction of additional functional building blocks for site-specific delivery, multimodal imaging, and enhanced therapeutic efficacy. Successful examples include well-known dyes, first of all tetrapyrroles (porphyrins and relative compounds), incorporated into a polymer matrix—such as Photofrin®-loaded ~40 nm diameter polyacrylamide

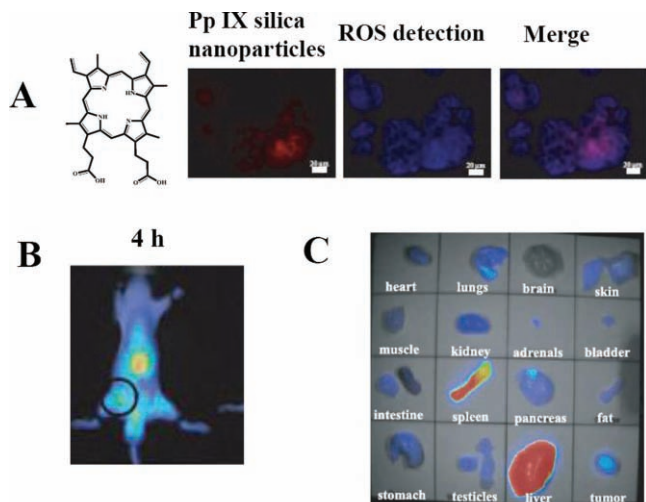


Figure 3. A) Cytoplasmic localization of Pp IX silica nanoparticles and of ROS liberation on HCT 116 cells. Colocalization between nanoparticles and ROS liberation (merge). B) In vivo imaging of biodistribution of Pp IX/dioctadecyl tetramethyl indodicarbocyanine chlorobenzene (DID) silica nanoparticles on glioblastoma multiforme Mouse xenografted model. C) Fluorescence of glioblastoma mouse model isolated organs: heart, lungs, brain, skin, muscle, kidney, adrenals, bladder, intestine, spleen, pancreas, fat, stomach, womb-ovary/testicles, liver and tumor, 24 h after intravenous injection. The tumor (but not brain itself) and the liver were the two tissue types showing the strongest nanoparticle-related fluorescence. Reproduced with permission.^[22] Copyright 2010, Wiley.

multifunctional particles,^[23] or 10–60 nm in diameter silica-encapsulated Protoporphyrin IX (Pp IX),^[22] PS encapsulated in a polymer matrix is passively internalized into the cellular cytoplasm and retains the capability of spatially-focused production of ROS, **Figure 3A**. In both reports,^[22,23] because of relatively low quantum yields of the dye PSs, additional functionalities—more efficient fluorescent labels (carbocyanine lipophilic tracer DID^[22] and Alexa Fluor 594^[23]) were also uploaded into polymer matrixes. Systematic biodistribution studies of Pp IX silica nanoparticles loaded with the DID tracer were carried out in three mouse xenografted human glioblastoma models.^[22] As shown in **Figure 3 B**, high tumor uptake of Pr IX silica nanoparticles loaded with DID tracer was observed 2 hours after tail vein injection, while a tracer not encapsulated in nanoparticles did not accumulate at the tumor site. With respect to healthy tissues, nanoparticle accumulation in the liver and spleen was much greater than within the tumor mass, as shown in **Figure 3C**. In addition, nanoparticles were not observed in the brain, indicating limited ability to cross the BBB and limited brain targeting. While the dye-silica nanoparticles tend to passively accumulate in the model tumor possibly due to the enhanced permeability and retention effect, this nanoplatform would benefit substantially either from the addition of targeting functionalities for controlled delivery or application of engineered implantable devices.

3.2. Metal Oxide and Metal Particles

The focus of this section is colloid metal oxide and metal photoactive nanoparticles—semiconductor TiO₂ nanocrystals and

gold nanoparticles. Both metal oxide and metal particles can be routinely surface-functionalized with hydrophilic polymers and biological moieties via catecholate/metal oxide^[19,24–27] or thiolate/gold chemistries. In addition to the well-known application benefits of nanoscale materials, such as high surface-to-volume ratios, compared to organic dye PSs (either bulk, or encapsulated into polymeric scaffolds) metal oxides and noble metal photoactive nanoengineered materials are chemically and photo-stable.

3.2.1. Titanium Dioxide

TiO₂ is a semiconductor with a relatively wide band gap of 3.2 eV (anatase), and is well-known as a ultraviolet light (UV)-inducible catalyst in the photooxidation of organic substrates and the deactivation of bacteria, algae, and viruses.^[28] Under UV excitation, TiO₂ nanoparticles of various sizes and morphologies have been reported to exhibit cytotoxicity toward some tumors.^[27,29] Furthermore, TiO₂-based colloid particles, and their composites, have been successfully applied for destruction of brain cancer cells.^[19]

One recent example^[27] describes 50 nm rhodamine-labeled TiO₂/PEG constructs able to be internalized into rat glioma C6 cells, **Figure 4 A**. Although the essential question regarding accumulation selectivity of the photocatalyst in cancerous cells over healthy astrocytes remains to be answered, the anti-glioma activity of these hydrophilic nanoconstructs was found to be remarkable. The antitumor performance was evaluated in glioma cell spheroids representing a provisional three-dimensional model valuable for translation to animal xenografted models. The cytotoxic effect of the UV-irradiated photocatalyst depended on the concentration of TiO₂/PEG and the light exposure time, as shown in **Figure 4B**. More than 90% of cells were

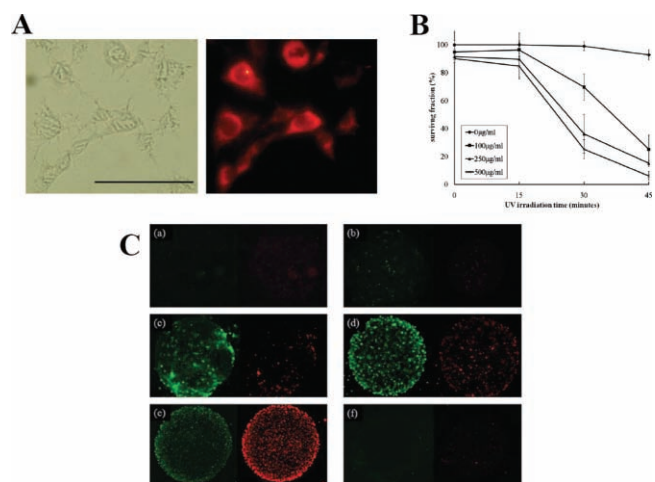


Figure 4. A) The optical transmission (Left) and fluorescence (Right) images of C6 cells internalized with rhodamine-labeled TiO₂/PEG. B) Surviving fraction of C6 cells as a function of UV irradiation in the presence of different concentrations of TiO₂/PEG (0, 100, 250, 500 µg/mL). C) Fluorescence photomicrography images of UV-irradiated C6 spheroids with TiO₂/PEG (a–e) and without TiO₂/PEG (f), co-stained with Annexin V-FITC (left)/propidium iodide (PI) (right); (a) before UV exposure, (b) immediately after UV exposure, and (c) 6 h, (d) 12 h and (e, f) 24 h after UV exposure. Reproduced with permission.^[27] Copyright 2010, Wiley.

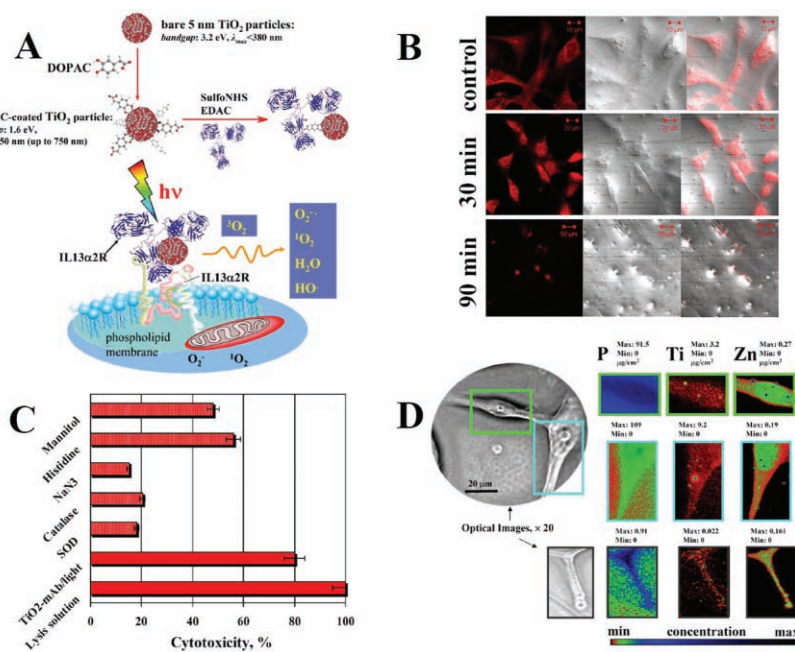


Figure 5. A) Modification of 5 nm TiO₂ semiconductor particles with electron donating enediol ligands results in narrowing the bandgap to 1.6 eV and red-shifting the absorption edge to the visible part of the solar spectrum. B) ROS cause cell membrane damage, permeability changes, and cell death. Only 5 min of white light illumination with intensity of 60 mW/cm² results in remarkable cell morphology changes. Laser confocal images of cells interfaced with the nanobio composite: control cells, 30 and 90 min following the light exposure. C) Photoexcitation of the nanobio hybrid in an aqueous solution results in the formation of various ROS. Cytotoxicity of the TiO₂-antibody hybrid is reduced in the presence of ROS quenchers, mainly superoxide anion. D) Direct visualization of the TiO₂-antibody/receptor interaction and mapping of the IL13R location and distribution throughout a single A172 brain cancer cell using synchrotron-based X-ray fluorescence microscopy. Reproduced with permission.^[19] Copyright 2009, American Chemical Society.

killed by a UV dose of 13.5 J cm⁻² in the presence of the nanocatalyst at a concentration of 0.5 mg/mL. The irradiated spheroids in the presence of TiO₂/PEG showed growth suppression compared with control groups, Figure 4C. Moreover, fluorescent images of the photocatalyst-treated spheroids co-stained with apoptosis and necrosis markers, Annexin V-FITC and propidium iodide (PI), reveal the prevalence of induced apoptotic cell death within first 6 hours (Figure 4C).

As shown schematically in Figure 5A, another work^[19] suggests approaches to resolve the two main concerns regarding the use of small TiO₂ nanocrystals in biological systems—non-specific distribution within cancer and healthy cells, and UV light photoreactivity. Although nanoscale materials tend to passively accumulate in tumors due to enhanced permeability and retention effects, and often serve as “nanocarriers” for chemotherapeutics, this passive strategy has limitations because of the risk of random delivery. The problem of passive transport can be improved by integrating hard inorganic nanomaterials with biological targeting vehicles—for example, an antibody. Functionalization of 5 nm high crystallinity TiO₂ nanoparticles with a monoclonal antibody recognizing IL13R (discussed in Section 2) fostered nanoparticle delivery specifically to glioblastoma cells in a manner dependent upon cellular membrane IL13R expression. Since visualization of 5 nm TiO₂ nanocrystals within cells

without additional labeling represents a challenge for conventional microscopies, direct visualization of the TiO₂-antibody/receptor interaction and mapping of the IL13R location and distribution throughout a single A172 brain cancer cell was demonstrated using synchrotron-based X-ray fluorescence microscopy, Figure 5 D.^[19,24]

PDT using the nanobio hybrid photocatalyst (at concentrations from 6–600 ng/mL) resulted in the destruction of over 80% of A172 glioma cells with high levels of IL13R expression, whereas in the case of U87 cells characterized by lower antigen presentation, cytotoxicity at the same conditions reached a plateau of ~50% and did not increase at higher photocatalyst concentrations. Moreover, no cytotoxicity was observed for normal human astrocytes (NHA) known to be not IL13R-expressing. It must be noted that 5 nm TiO₂ nanocrystals not functionalized with an antibody demonstrated slight (<20%) non-specific light-driven toxicity for all types of cells; this fact must be considered when any small nanoparticles are applied to biological systems.^[19,24]

Another challenge for bioapplication of TiO₂ semiconductor nanocrystals is in tailoring of the photochemical properties and extending reactivity toward the visible light region. While common approaches for shifting TiO₂ reactivity include doping inorganic elements—for example, rare earth ions—another method developed by T. Rajh and colleagues^[24–26] is based upon chemisorption of

organic molecules, such as dihydroxybenzenes (e.g. dopamine, DA), upon the surface of the semiconductor particles. As a result of the presence of two OH- groups in the ortho position, the catecholate group forms a strong bidentate complex with coordinatively unsaturated Ti atoms at the nanoparticle surface. It has furthermore been shown that DA creates electronic coupling between TiO₂ and DNA, allowing transport of photogenerated holes to biomolecules.^[25] Modification of TiO₂ particles with electron-donating enediol ligands results in significant improvements to the outer crystal structure and photo-reactivity of the particles, narrowing the band gap to 1.6 eV and red-shifting the absorption edge to the visible part of the solar spectrum below ~750 nm.^[30] As can be seen in Figure 5 B, the application of polychromatic visible light, with an incident intensity of 60 mW/cm² for 5 min duration, with UV and IR cutoff wavelengths filters, led to instant morphological changes in A172 cells.

It is well established that UV-photoexcitation of bare TiO₂ particles in aqueous solution results in the formation of various ROS, mainly hydroxyl (OH), peroxy (HO₂) radicals, and singlet oxygen (¹O₂).^[31] However, in the case of DA- and DA-antibody- modified TiO₂ particles, ROS arise from multiple, mechanically distinct redox chemistries, and the principal ROS produced is the superoxide anion, formed by reaction of photogenerated electrons with

molecular oxygen.^[26] Further *in cellulo* studies of photo-induced cytotoxicity toward A172 glioma cells in the presence of selective ROS quenchers were consistent with these results, as shown in Figure 5 C.^[19] Induced apoptosis was proposed as a foremost pathway in TiO₂-DOPAC-antibody-catalysed cell phototoxicity.^[19]

Nanostructured porous TiO₂ has been developed as a biocompatible nano-device for constant chemotherapy drug release into the CNS.^[31a-c] A porous titania carrier uploaded with low concentrations of a cytostatic platinum complex was capable of inducing DNA fragmentation, possibly via a strong interaction between nitrogen atoms in nucleotides, and Lewis acid sites on both the titania surface, and the platinum complex coordination sphere. Application of this material directly on to C6 glioma xenografted into Wistar rats resulted in a significant decrease in tumor size and growth rate. Although no light stimulus was employed in these trials,^[31a-c] they are included in this section since a photo-reactive material served as the scaffold for release of a cytostatic agent. The overall potential of this porous material remains to be explored in combined brain cancer chemo- and photo-therapies.

3.2.2. Gold Nanoparticles

Owing to unique photophysical properties, resistance to photobleaching, well-established control over the surface chemistry and biocompatibility gold nanostructures with variety of geometries, sizes and structure (solid, hollow, core-shell) represent important class of materials for simultaneous photothermal treatment and molecular imaging of cancer. Distinct optical properties of gold nanomaterials can be engineered to either strongly absorb or scatter light within the visible to near-infrared (NIRF) wavelengths (650–950 nm) which correspond to the “optical transmission window” of the biological tissues. Photophysical properties of these materials can be tuned by tailoring the core diameter and shell thickness of the gold nanoshells,^[32] aspect ratio of the rod-shaped gold particles^[33] or size and composition of porous-walled hollow nanocages.^[34]

Photothermal ablation therapy is based upon application of gold “nanoheaters” able to absorb laser light near their plasmon resonance band, with subsequent heat generation. Thus, plasmonic nanoshells consisting of a dielectric silica core encapsulated in a thin metallic gold shell represent a prospective class of optically tunable nanoparticles.^[35,36] The construction of immunonanoshells through grafting of specific antibodies to the nanoshell surface allows spatial control of heat dissipation, destroying only cancer cells and leaving healthy tissues intact. This approach was successfully applied *in vitro* to medulloblastoma and two high-grade glioma U373 and U87 cell lines.^[18] Nanoparticles with ~100 nm silica cores and 10 nm gold shells, which were optimized for peak light absorption at 800 nm, were conjugated with PEG linkers and then functionalized with antibodies to HER2 and IL13R antigens, which are specifically over-expressed on the surfaces of medulloblastoma and glioma cells, respectively. While bare nanoshells were absorbed to cells non-specifically and, under laser application, induce cell death, their PEG-conjugated analogues did not bind to cells, and were not toxic. Finally, only nano-bio hybrid immunonanoshells were able to destroy brain cancer cells specifically.

Authors from California^[37] demonstrated significant photothermal effect of supramolecular nanoparticles (SNPs)

self-assembled from β -cyclodextrin (CD) and adamantane (Ad) building blocks with embedded 2 nm Au toward U87 glioblastoma cells. Specific targeting to $\alpha(v)\beta(3)$ integrin receptor was attained by incorporation of target-specific RGD peptide ligands to the SNPs. Interesting that enhanced phototoxicity of these Au-SNPs in comparing with original 2 nm Au colloid particles can be connected with formation of explosive microbubbles capable of mechanical destruction of cancer cell.^[37]

Gold nanorods were proposed for photothermal therapy and dark field light scattering imaging as well.^[38] Gold nanorods of aspect ratio of 3.9 linked to the EGFR-specific antibody were observed to cause photothermal destruction of malignant HOC 313 clone 8 and HSC 3 (human oral squamous cell carcinoma) cells under exposure to a near-infrared laser at 800 nm. Although this approach was successfully demonstrated to be applicable in oral and head and neck cancers it probably can be used for other solid tumors which over-express EGFR, including brain cancer.

In addition to thermal therapy, gold nanostructures demonstrate great potential in imaging in diagnostics serving as molecular contrast agents. Because of high extinction coefficient gold nanoparticles can be utilized as contrast agents for dark field, light scattering, and two-photon luminescence imaging. Moreover, gold nanomaterials were used for signal amplification in photoacoustic tomography (PAT), PAT is an advanced diagnostic hybrid technique based on laser-induced thermoelastic expansion through biological tissue which allows combining benefits of optical and ultrasound imaging.^[39,40] PAT allowed non-invasive *in vivo* molecular imaging of living small animal brain vascular system^[39] and, even more, imaging of important hallmarks of a tumor development and progression such as angiogenesis^[41] and hypoxia.^[42] Wang and coworkers applied PEGylated gold nanoshells as exogenous NIR contrast agent for laser-induced PAT of the rat brain *in vivo* with high spatial resolution and satisfactory sensitivity.^[43] Later this approach was advanced by application of PEG-coated gold nanocages of more compact size of 50 nm and large optical absorption cross section.^[44] Further, Lu et al. used PEG-shielded 40 nm mesoscopic hollow gold nanospheres (Figure 6) for PAT-mapping of living mouse brain vasculature.^[45] The image depicted brain blood vessels as small as ~100 μ m in diameter using the nanospheres as contrast agents as shown on Figure 6. In addition, preliminary results revealed no acute toxicity to the liver, spleen, or kidneys in mice following a single imaging dose of the hollow gold particles.

In overall, PAT approach is very promising technology for brain tumor vasculature-targeted imaging and, further, for targeted anti-angiogenic therapy.

Based to well-known ability of gold to induce a strong X-ray attenuation Kopelman and coworkers suggested to utilize gold nanorods as contrast agents for X-ray computed tomography.^[46] Using the UM-A9 antibody for functionalization of gold nanorods they demonstrated an *in vitro* proof of principle for effective targeted imaging of head and neck cancer.

4. Magnetic Materials

Since the discovery of the compass, magnetic phenomena have been an essential facet of everyday life, most markedly in recent

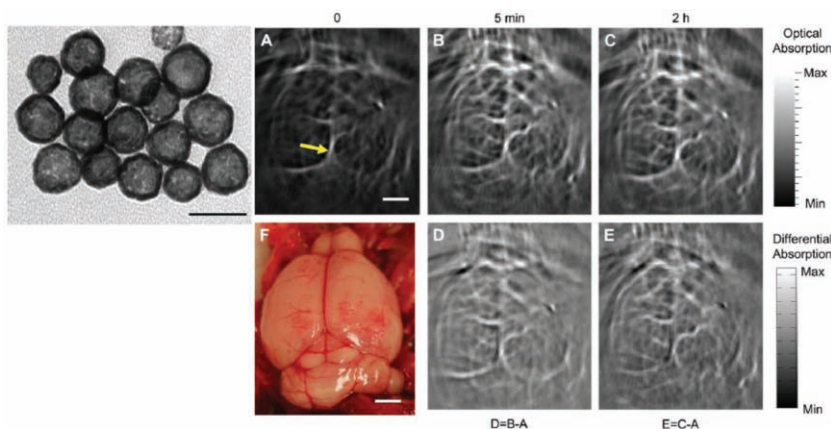


Figure 6. Left: hollow gold nanospheres (TEM image, bar = 50 nm). Right: noninvasive PAT imaging of a mouse brain in vivo employing PEG-HAuNS and NIR light at a wavelength of 800 nm. Photoacoustic image acquired (A) before, (B) 5 min after, and (C) 2 h after the intravenous injection of PEG-HAuNS. (D) and (E) Differential images that were obtained by subtracting the pre-injection image from the post-injection images. Arrow, middle cerebral artery. Bar = 2 mm. (F) Open-skull photograph of the mouse brain cortex obtained after the data acquisition for PAT. Bar = 2 mm. Reproduced with permission.^[45] Copyright 2010, Elsevier.

times with magnetic recording and advanced information technologies. In the life sciences and in the field of advanced medical technologies, magnetic nanoparticles provide an unprecedented level of functionality. Life sciences applications include magnetic resonance imaging (MRI) contrast enhancement, targeted and triggered drug delivery and release, bioseparation, magnetofection, and magnetically induced hyperthermia.^[47–49] Magnetic nanoparticle preparation, functionalization in solution, and their application to biomedicine were comprehensively summarized in recent excellent reviews.^[50–53] Innovative methods of magnetic actuation have recently been explored for the distant control and manipulation of cell adhesion, receptor clustering, and intercellular signaling.^[55,56]

4.1. Superparamagnetic Particles

4.1.1. Hyperthermia

Magnetic fluid hyperthermia has been known for over 50 years.^[57] This therapy is based upon the ability of magnetic nanoparticles to resonantly respond to alternating (*ac*) magnetic fields. Targeted to cancer tissues and exposed to *ac* fields, these particles act as a localized heat source, elevating the temperature of the surrounding tumor to cytotoxic levels.^[50,51] In spite of the dynamic growth of innovative nanoplatforms—from the design of smart functional materials, to translational research with a focus on clinical application—the path from bench-to bedside is still challenging, extensive, and multi-faceted. At present, in the field of advanced materials for brain cancer imaging and therapy, the most remarkable progress toward clinical trials (phase II, efficacy study) has been achieved with superparamagnetic nanoparticles.^[3] A group from Germany has been developing a first-ever clinical method of therapeutic magnetic hyperthermia. The foremost target of this therapy is glioblastoma. Therefore, for the first time the feasibility of using

magnetic nanoparticles for hyperthermia in human patients has been demonstrated for brain cancer. In 2006, this group reported that hyperthermia using aminosilane coated superparamagnetic iron oxide nanoparticles, with an average core diameter around 15 nm (a “magnetic fluid”), caused a significant (up to 4.5-fold) prolongation of survival in glioma-bearing rats.^[3a] Shortly thereafter, the same group demonstrated the efficiency of the hyperthermia combined with radiotherapy in a study involving 14 patients with recurrent glioblastoma multiforme.^[3b] The amount of the magnetic fluid, and its spatial distribution, were planned in advance using specially developed 3-dimensional computer software for treatment simulation, as seen in Figure 7 A. For calculation of the expected heat delivery within the tumor, the distribution of the implanted nanoparticles was measured by computed tomography (CT) and matched to MRI images taken preoperatively, Figure 7 B. By solving the heat transfer

equation, the temperature distribution is derived from the magnetic field strength *H* (actually applied during treatments), the nanoparticle density in the specific region (calculated from the density distribution in the CT), and the nanoparticle specific absorption rate. Hyperthermia was performed in an *ac* field of 100 kHz frequency, with variable field strength between 2.5–18 kA/m. Although patients’ survival has not yet been reported, safe application of hyperthermia and the potential to controllably apply hyperthermic temperatures (42.4–49.5 °C) in human patients was demonstrated. Currently, the efficacy of the method is under evaluation on a group of 65 patients in a phase II trial, which is expected to provide an initial indication whether magnetic hyperthermia can improve survival and quality of life.^[3c] Additionally, post-mortem neuropathological studies of glioblastoma patients who received the hyperthermia are currently under meticulous study.^[3d] These detailed studies are essential to determine the distribution and fate of nanoparticles in the human brain, as well as to examine whether the hyperthermia has adverse effects.

4.1.2. MRI Contrast Enhancement

MRI with nanoparticles exploits the magnetically dephased signal from water molecules surrounding biological tissue labeled with magnetic nanoparticles excited by radiofrequency waves in a strong magnetic field.^[58] Iron oxide nanoparticles have been approved by the Food and Drug Administration (FDA) for use for MRI contrast enhancement.^[59] In neurooncology, they have been utilized as MRI contrast agents to improve the differentiation of neoplastic from normal brain tissue.^[60,61] In comparison to conventional gadolinium chelates, contrast agents based upon magnetic nanoparticles offer improved demarcation of tumor margins—most likely owing to enhanced permeability and retention—which may lead to more positive surgery outcomes.^[60,62] It is obvious that MRI enhancement with superparamagnetic particles

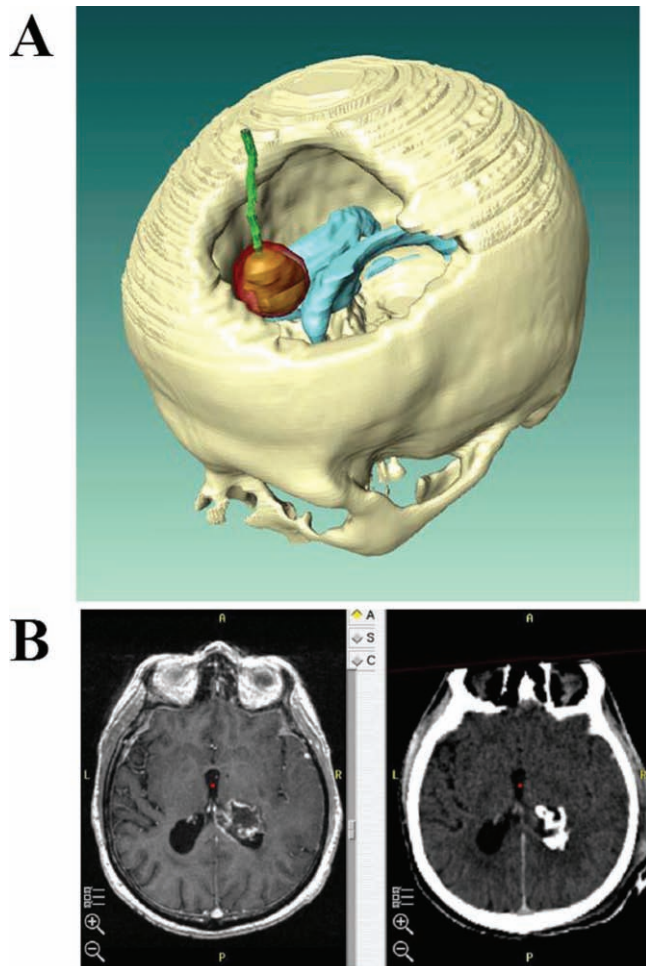


Figure 7. A) Three-dimensional reconstruction (MagForce NanoPlan software) of a skull with a frontal glioblastoma multiforme after magnetic resonance imaging and computed tomography. Calculated 42 °C treatment isotherm surface (transparently red) enclosing the whole tumor (brown), thermometry catheter (green), ventricle (light blue). B) Preoperative MRI with glioblastoma multiforme infiltrating the right posterior horn of the ventricle (left). The postoperative CT shows the magnetic nanoparticles as hyperdense areas within the tumor tissue (right). Reproduced with permission.^[3b] Copyright 2007, Springer.

would benefit from the use of entities targeting tumors and biological barriers. For this reason, 10–15 nm amine-terminated PEG-coated iron oxide particles have been linked to a targeting agent, chlorotoxin (CTX). CTX, a 36-amino acids peptide originally isolated from the venom of the *Leiurus quinquestriatus* scorpion, demonstrates a high affinity to the membrane-bound matrix metalloproteinase-2 (MMP-2). MMP-2 is specifically over-expressed by malignant cells, including glioma and medulloblastoma.^[63] CTX-functionalized PEG-coated nanoparticles have demonstrated great potential as MRI contrast agents specifically recognizing brain tumors, both in 9L cells and in a mouse xenografted tumor model.^[63] As Figure 10 clearly demonstrates, a targeted CTX-functionalized nanocomposite exhibits superior potential for precise tumor imaging compared with nanoparticles without the targeting peptide.

A similar approach has been successfully employed by another group.^[64] This approach uses a membrane-permeant contrast agent consisting of a superparamagnetic iron oxide core conjugated to a polycationic lipopeptide (β -Ala(Mys)-Arg-Arg-Arg-Arg-Arg-Arg-Arg-Cys-NH₂) as a membrane translocation module. The agent is labeled with the NIRF dye Cy5.5 for correlative microscopy. This nanoconstruct showed a remarkable uptake by U-87 human glioma cells in vitro, and a localized and delineated MRI signal when stereotactically injected into a tumor in vivo.

In related work, another group of authors employed the encapsulation of superparamagnetic particles within a polymeric scaffold.^[65] In general, this strategy enables the production of magnetic spheres with high magnetic moments. Iron oxide nanoparticles coated with a PEGylated amphiphilic triblock copolymer (consisting of polybutylacrylate, polyethylacrylate, polymethacrylic acid, and a hydrocarbon hydrophobic chain) were conjugated with a NIRF fluorescent dye and cyclic Arginine-Glycine-Aspartic acid containing peptide c(RGDyK) for the purpose of integrin $\alpha(v)\beta(3)$ targeting. Successful tumor homing in vivo was perceived in a subcutaneous U87MG glioblastoma xenograft model by both MRI and NIRF imaging. Moreover, ex vivo histopathological studies revealed low particle accumulation in the liver.

4.2. Magnetic Materials Microfabricated by Physical Methods

While the majority of reports on biomedical applications of magnetic materials deal with chemically synthesized superparamagnetic particles with sizes in the range of tens of nm, advanced systems based on ferromagnets are also of great interest. Instead of solution-based assembly, these materials are lithographically-defined using top-down techniques, such as micro- and nano-fabrication combined with physical vapor deposition, followed by release and stabilization in solution. This approach allows the fabrication of monodisperse particles of virtually any shape, including multicomponent and multilayered materials, with tunable magnetic properties (including high saturation magnetization and zero remanence due to in-plane or out of plane flux closure), and sizes down to ~100s nm. For example, such magnetic materials are used in super-sensitive giant magnetoresistance spin valve or magnetic tunnel junction sensors capable of detecting minute concentrations (down to picomolar) of DNA and proteins in vitro,^[66,67] as advanced MRI enhancement agents,^[68,69] and in magnetofection.^[70]

Recently, antibody-functionalized ferromagnetic disks were successfully interfaced with N10 glioblastoma cells.^[4] Because the particles are flat, their magnetic moments are arranged in a unique pattern known as a spin vortex state (see **Figure 8**). The disks are 50 nm thick, 1 μ m in diameter, and composed of a 20:80% iron-nickel (permalloy) magnetic core encapsulated in 5-nm gold shell (Figure 8 G). The particles were prepared by optical lithography and magnetron sputtering with following release to aqueous solution, Figure 8 A–G. Owing to their anisotropic shape, the magnetic particles respond to an external applied magnetic field with a mechanical torque, similar to how a compass needle aligns with the Earth's field. Therefore, the magnetic disks function as mediators to deliver the energy of

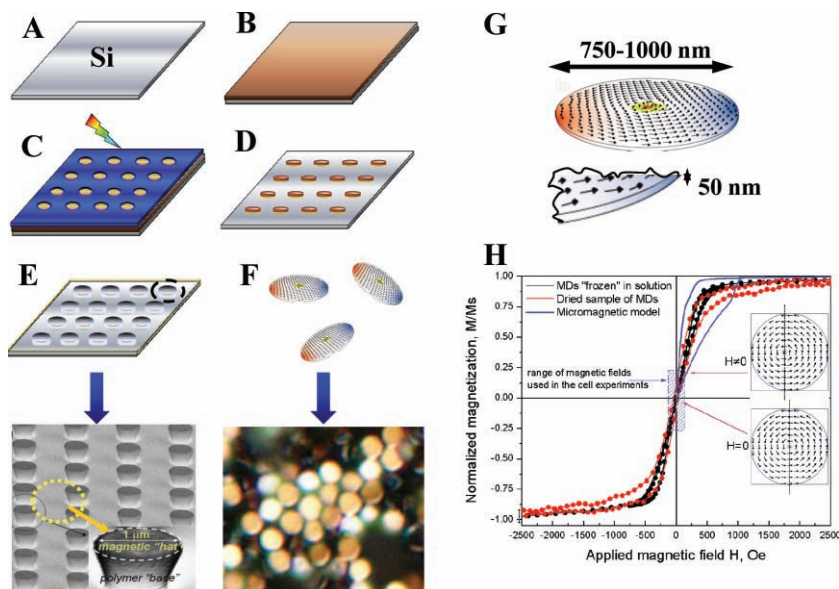


Figure 8. Ferromagnetic disks possessing vortex ground state. A–F) Disks fabrication: The process starts with photoresist spin coating and developing (B) on a silicon wafer (A). A mask is placed in contact with the layer of pre-baked photoresist and illuminated with UV light (C). An organic solvent dissolves and removes photoresist that is not exposed (D). Finally, magnetron sputtering is used to deposit a 5 nm underlayer gold, followed by 40 nm of the iron-nickel permalloy, and topped with another 5 nm of gold layer (E and an optical micrograph below). The disks are released from the wafer by lift-off process in acetone (F and an optical micrograph below). G. Vortex spin arrangement in remanence is the characteristic ground state for magnetically-soft geometrically confined planar structures (magnetic core diameter 800 nm and thickness 40 nm). H) A room temperature magnetic hysteresis loop for a dried sample (red symbols) measured with VSM and MDs in acetone solution cooled in presence of 50 Oe magnetic field below freezing point of -95°C (black symbols). The dashed blue area depicts the magnetic field range used in the cell experiments. Reproduced with permission.^[4] Copyright 2010, Nature Publishing Group.

an external source (the magnetic field) to the cell membrane via a magneto-mechanical coupling. Similar to other reports,^[16–19] this approach utilized an anti-IL13R antibody to specifically attach to the antigen over-expressing N10 cells. The application of *ac* fields of 90 Oe and 10–20 Hz frequency for only 10 min resulted in drastic cell morphology and biochemistry changes, including the loss of membrane integrity and nuclear material re-distribution, **Figure 9 A**.

Cytotoxicity assessed by an LDH test reached its maximum of ~90% at low frequencies of the applied magnetic field, from 10 to ~20 Hz. Furthermore, significant magneto-mechanical stimulus-induced nuclear DNA damage was revealed using the TUNEL assay, as shown in B. TUNEL staining was remarkably (~50%) inhibited by addition of Z-VAD-FMK (carbobenzoxy-valyl-alanyl-aspartyl-[O-methyl]-fluoromethylketone), an inhibitor of caspase proteases, the key enzymes in apoptosis. The magnetic-vortex induced forces applied to the cell surface were calculated to lie in the range of ~10s of pN range, while much higher (>100s pN) forces are typically needed to physically rupture the cell membrane. However, forces as small as a few pN have been reported to be sufficient to activate a single ion channel, or to create a pore in the cell membrane comparable in diameter to its thickness. In addition, it is well-established that disturbances in the membrane integrity can change the calcium equilibrium

and induce apoptosis. This proposed mechanism of membrane channel actuation or/and pore formation was confirmed through real time laser confocal imaging of intracellular calcium using the calcium indicator Fluo-4AM. Under *ac* field application the calcium level in studied cells increased, and dynamic oscillations, spikes and relocalization of calcium were observed, as shown in Figure 9 C. Benefits of the proposed approach include the utilization of unprecedentedly low frequency *ac* fields for triggering cancer cell apoptosis via direct energy transfer to a single cell, and the transformation of magnetic field-induced mechanical forces to ionic current signals. It is not known yet whether this concept could also be efficiently applied in vivo for other types of cancer. Although targeting of a nanomaterial to different antigens specifically over-expressed on malignant cells is quite straightforward, one must consider that glioblastoma abnormally derives from glial cells. Glial cells use calcium for intercellular communication, and are therefore important function intrinsically very susceptible to changes in calcium homeostasis. On the other hand, while the above results were obtained using ~1 micron diameter disks, the concept could be scaled down to ~100 nm dimensions. If hybridized with soft material such as polymer matrix the ferromagnetic disks-based approach can be expanded to engineering of mechanoresponsive microdevices for tunable and controlled drug release.^[71]

5. Multifunctional Materials

Multi-functionality and multi-capability is a hallmark of nano-platform concept. Owing to the literally endless possibilities to integrate polyvalent entities into a sole supreme material offered by nanoscale approaches, a number of recent publications describe composite materials in which every component of a hybrid plays an equally significant role in biorecognition and targeting, multimodal imaging, and therapy. While nanoparticles such as iron oxide and gold are recognized to have extraordinary diagnostic and therapeutic potential, quantum dots (QDs), or semiconductor nanocrystals, are suitable for bioimaging, including in vivo fluorescence imaging and *ex vivo* immunofluorescence.^[72] In addition to inorganic nanoparticles, polymeric nanoparticles and dendrimers have been explored extensively for the same purposes.^[73] Interfacing between inorganic nanocrystals and biological molecules such as proteins, leader peptide sequences, and nucleic acids (aptamers, siRNA) results in new materials -multivalent hybrids with synergistically enhanced properties, which may serve as platforms for brain cancer diagnostics and treatment. Although some of the following examples could perfectly fit previous sections of this report (e.g. photoactive or magnetic materials), these hybrids

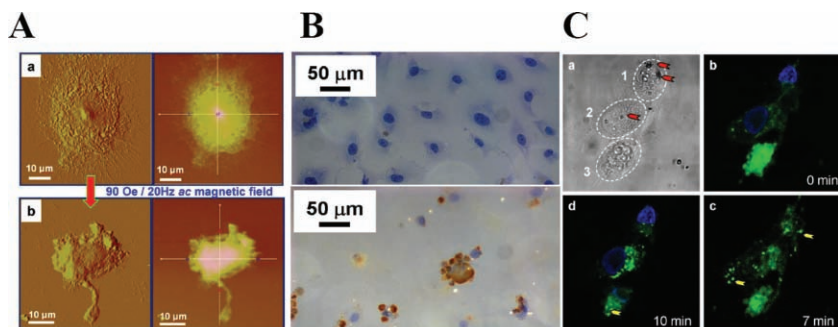


Figure 9. Magnetic-vortex-mediated mechanical stimuli trigger intracellular biochemical pathways activating programmed cell death. A) Comparison of representative AFM amplitude error, height and cross-section scans for the control (a) and treated cells (b). B) Biofunctionalized ferromagnetic disks attached to N10 glioblastoma cells (control cells, top) and the same cells subjected to 20 Hz–90 Oe ac fields for 10 min and TUNEL stained 4 h after the magnetic-field exposure (bottom). C) Magnetic-vortex mediated mechanical stimuli are converted and amplified into a Ca^{2+} ionic signal and apoptosis initiation. The N10 cells were preloaded with calcium indicator Fluo-4-AM, green, whereas cell nuclei were stained with Hoechst 33342, blue. Subpanel a) Cell optical images. Subpanels b–d) Fluorescent cell images: snapshots at 0, 7 and 10 min application of alternating magnetic field of 10 Hz–90 Oe. Yellow arrows show representative calcium flashes or spikes. Reproduced with permission.^[4] Copyright 2010, Nature Publishing Group.

are nominally classified as multifunctional materials and discussed in this section.

5.1. Hybrids with Magnetically and Optically Active Components

A 2006 report from a group from Michigan^[23] represents an archetype for the brain cancer multifunctional theranostics nanoplatform. Polyacrylamide nanoparticles consisting of encapsulated PS (Photofrin) and multimodal imaging agents (iron oxide and NIR Cy5.5) were functionalized with the tumor vascular homing peptide F3 through hydrophilic PEG linker. The F3 is a 31 amino acids peptide (KDEPQRSARLSAK-PAPPKPEPKKAPAKK) discovered throughout phage display screening that able to penetrate the tumor intravascular space. Therefore, the multicomponent construct was evaluated in vitro for its ability to produce singlet oxygen, target the nucleolin cell surface receptor (a specific marker within the tumor vasculature), and confer photosensitivity. In vitro studies revealed that F3-targeted nanoparticles were targeted to cancer cells, and then internalized and concentrated within tumor cell nuclei. Subsequent nanoparticle photoactivation resulted in the loss of cell viability. Moreover, in vivo studies revealed that these multifunctional nanoparticles were detectable in 9L glioma-bearing animals using MRI. Administration of laser light to the tumor site through a fiber optic applicator increased survival time, which is a significant therapeutic benefit. Furthermore, F3-targeted nanoparticles were more efficient than both non-targeted nanoparticles, or Photofrin alone. Similar strategies based upon combinations of magnetically and optically active components with polypeptide entities for targeting brain cancer were also reported by other groups.^[63,74] Although these multimodal systems were applied for delineation of cancerous regions either through MRI enhancement or

fluorescent imaging, in principle they may be applied for cancer treatment via magnetic hyperthermia.

In addition to polypeptide-based carrier systems, at the present time biomolecules with low molecular weights, known as aptamers, are becoming popular building blocks for engineering of advanced multifunctional systems at nanoscale. Aptamers are short synthetic single-stranded DNA or RNA oligonucleotides that bind with high affinity to target molecules.^[75] Recently, a high precision aptamer-based probe panel for identification of the primary human glioma cell lines was developed.^[76] Similar to earlier work,^[23] authors from Korea^[77] have reported on in vitro and in vivo targeting of multimodal nanoparticles to the same nucleolin antigen using an aptamer-based approach. Cobalt–ferrite nanoparticles surrounded by fluorescent rhodamine tracers within a silica shell matrix were covalently linked to a 5'-NH₂-modified AS1411 aptamer (5'-TTGGTGGTGGTGGTGGTGGTGGTGGTGG-3'). These nanoparticles were additionally functionalized with 2-(p-isothiocyanatobenzyl)-1,4,7-triazacyclonane-1,4,7-triacetic acid (NOTA) as a chelating agent and radio-labeled with the radioisotope ⁶⁷Ga for scintigraphic in vivo imaging, as shown in Figure 10. Successful targeted delivery of these multimodal nanoconstructs was demonstrated using fluorescent, radioisotope and MRI modalities in vitro and in C6-bearing nude mice.^[77]

Aptamer-based targeting systems can also include semiconductor nanocrystals. For instance, owing to their excellent photochemical stability, high brightness and tunable spectral characteristics, semiconductor QDs are an attractive alternative to organic fluorophores. The outstanding properties of QDs are outweighed by their poor biocompatibility, which is most probably caused by the leaching of toxic Cd⁺.^[78] This problem could be reduced by application of core-shell nanocrystals^[79] or introduction of a polymeric shield. For example, the aptamer GBI-10 (which is specific to tenascin-C, an extracellular matrix protein over-expressed on the surface of glioma cells) was covalently linked to core-shell CdSe/ZnS QDs^[80] and CdSe nanocrystals together with a functional polyamidoamine (PAMAM) dendrimer.^[80,81] The resulting hybrid “nanoprobes” demonstrated excellent characteristics, including strong fluorescence, stability, monodispersity, and uniformity, and were applied for imaging of U251 glioblastoma cells.

While the application of QDs for fluorescent labeling is quite well-known, their ability to transfer electrons and holes to biomolecules—leading to spectral changes and to effects on living systems—have yet to be exploited. For instance, QDs linked to electron donor molecules can exhibit phototoxicity through the generation of ROS (singlet oxygen and hydroxyl radicals). This toxicity can be decreased by antioxidants.^[82] Recent work on QDs linked to catecholates suggests designs for bifunctional agents for both redox-specific labeling and PDT.^[82]

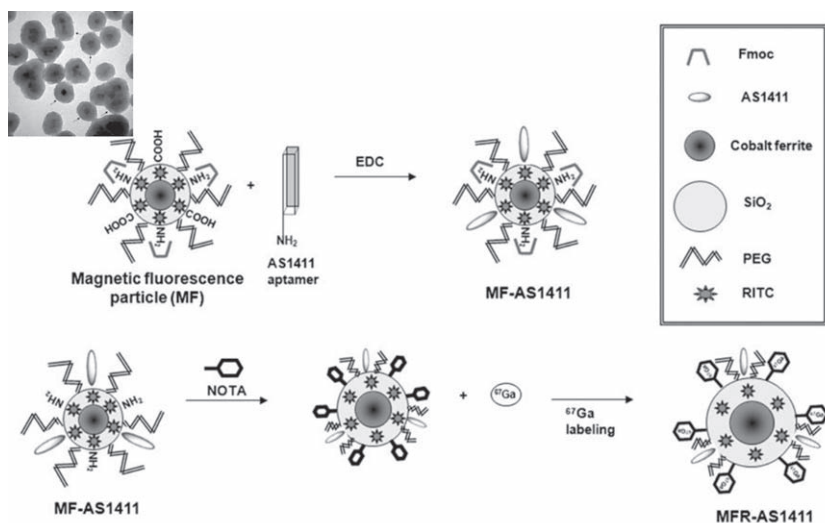


Figure 10. Scheme of preparation of the MFRAS1411. MF particles had carboxyl group and Fmoc-protected amine moiety, which was coupled with amino group terminated AS1411 aptamer using EDC (MF-AS1411). After reaction of MFAS1411 with p-SCN-bn-NOTA, particles were reacted with ^{67}Ga -citrate to form MFR-AS1411. Inset: TEM images of magnetic cobalt ferrite core, rhodamine dye, and MFR-AS1411; uranyl acetate (2%) was used to stain the AS1411 aptamer. Scale bar is 50 nm. Reproduced with permission.^[77] Copyright 2010, Society of Nuclear Medicine.

5.2. RNA Interference Multicomponent Multifunctional Platforms

Other multifunctional materials utilize advanced (RNAi)-based strategies, wherein small (~20–25 nucleotides) double-stranded RNA molecules capable to mediate cleavage of complementary mRNA sequences and thus inhibit the expression of targeted oncogenes.^[83] Since siRNAs are negatively charged and cannot freely travel to the cytoplasm of target cells, the full potential of this approach requires delivery of siRNA molecules to tumor cells in functional form as well as to monitoring of both siRNA delivery and the resulting knockdown effects. Using this approach, an application of multifunctional siRNA–QD constructs for selective inhibition of the EGFRvIII expression in human U87 glioblastoma was recently reported.^[84] As mentioned in Section 1, genes expressing epidermal growth receptor (EGFR) variant III deletion mutant (EGFR vIII) are an important target for novel brain cancer therapies. EGFRvIII is the key growth factor receptor triggering proliferation of cancerous cells. It is expressed in human GBM and in several other malignant cancers, but not in normal healthy cells.^[85] Knockdown of this gene is one of the most effective means by which to down-regulate the PI3K/Akt signaling pathway, which is a key signal cascade for cancer cell proliferation and apoptosis.^[86] As shown in **Figure 11**, core–shell CdSe/CdS/ZnS QDs with 7 nm diameter were derivatized with hydrophilic amine-terminated poly(ethylene glycol) and conjugated to siRNA through two types of linkers. One linker, 3-(2-pyridyl)-dithiopropionic acid pentafluorophenyl ester (PTPPf), was designed to release siRNA upon entering the cell by enzymatic cleavage of the disulfide bridge, while the other, non-cleavable linker, 3-maleimidopropionic acid pentafluorophenyl ester (MPPF), was designed for evaluation of cellular uptake and localization

of the siRNA construct within the cellular compartments, as shown in **Figure 11**. Furthermore, two peptides—RGD and HIV-Tat—were utilized as vehicles for enhanced cellular targeting and membrane transduction of the multifunctional construct. In vitro experiments with the U87-EGFP cell line revealed specificity of the siRNA against EGFRvIII, inherent noncytotoxicity of the QDs, and the usefulness of this multifunctional QD–siRNA approach for manipulation of cancer cell proliferation.^[84]

Another multifaceted hybrid containing magnetically- and optically-active components was successfully utilized for siRNA delivery to brain cancer, both in vitro and in a mice model.^[87] Magnetofluorescent “nanoworms” or “dendriworms” composed of a core of magnetic nanoparticles (the “worm”) were functionalized with branched cationic PAMAM dendrimers via a reducible linker, and labeled with a fluorescent tracer. Leveraging the electrostatic interaction, the polycationic dendrimer modules then were loaded with negatively charged siRNA. The resulting poly-

plexes were employed for targeted delivery and release of their siRNA cargo to glioma. Specific and significant suppression of EGFR expression levels was demonstrated in glioblastoma experiments, both in vitro and in transgenic animal models. Dendriworms were well-tolerated after seven

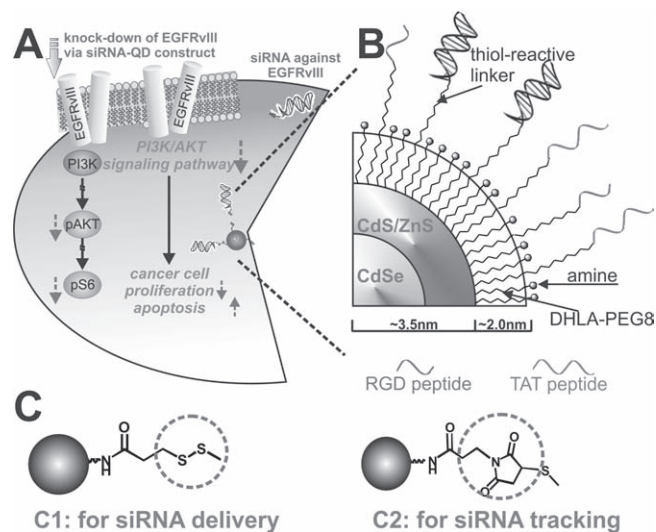


Figure 11. A) Quantum dots as a multifunctional nanoplatform to deliver siRNA and to elucidate the EGFRvIII-knockdown effect of PI3K signaling pathway in U87-EGFRvIII B) Detailed structural information of multifunctional siRNA–QDs. C) Two different strategies for the siRNA–QD conjugate. L1 shows the linker for attaching siRNA to QDs through a disulfide linkage which is easily reduced within the cells to release the siRNA. L2 shows the linker for covalently conjugating siRNA to QDs which enables the tracking of siRNA–QDs within the cells. Reproduced with permission.^[84] Copyright 2010, Wiley.

days of convection-enhanced delivery to the mouse brain. This report can serve as an example demonstrating how combination of advanced delivery, multimodal imaging, and targeting capabilities within the dendriworm platform offers a versatile and powerful tool to combat malignant glioma.

6. Delivery to Brain Cancer: Nanoparticle Administration and Application of External Stimulus

The delivery of drugs and other molecules across the intact BBB to the CNS represents a serious challenge. Nanoparticles have the potential to cross the BBB,^[88] a natural protective interface between circulating blood and the brain maintained by the tight junctions between endothelial cells. A layer of endothelial cells lining the capillaries in the brain restricts the diffusion of microscopic matter and hydrophilic pharmaceutical substances to the brain.^[89] However, in the case of brain neoplasms, the endothelial barrier can be compromised and show significant leakiness.^[90] For example, as demonstrated with the U87 glioma model, breakdown of the BBB can lead to the formation of pores 7–100 nm in size, sufficient to allow the translocation of certain nanoparticles.^[91] While the size of nanoparticles is the principal factor affecting the permeability of the BBB,^[88] surface charge and the additional surface functionalities designed into advanced materials can enhance their ability to cross the BBB, allowing them to manifest the imaging capabilities or therapeutic efficacy. Examples of advanced materials suitable for transport across the BBB include nanoparticles coated with Polysorbate 80 (Tween 80, T-80),^[92] liposomes,^[93] and functionalized dendrimers.^[73,94] However, the possibility of adverse effects resulting from nanoparticles crossing the BBB, including disruption of its protective function, remain to be meticulously evaluated before the safe application of nanoscale materials can be assured.

In the case of aggressive brain cancers, such as malignant glioblastoma and medulloblastoma (WHO grades III and IV), characterized by poor survival prognoses,^[9–12] anatomical (cranium) and physiological (BBB or blood tumor barriers) blockages can be bypassed rather than crossed. The most common scenario in the treatment of glioma includes maximal surgical resection of the tumor, followed by radio- and chemotherapy.^[12] Adjuvant chemotherapy includes the application of alkylating agents, such as temozolomide, or the implantation of a polymeric Gliadel® (14 mm in diameter and 1 mm thick) wafer directly into the surgical cavity for the purpose of steady drug delivery.^[12] Therefore, in the treatment of such forceful cancer, when surgery is imperative, therapeutics can be directly delivered to the brain tumor. For example, convection enhanced delivery (CED) is a powerful method which allows the continuous delivery of therapeutic agents under positive pressure directly to the CNS while bypassing biological barriers through catheters implanted during surgery. Designed for the delivery of macromolecules which would otherwise not cross the blood-brain barrier into the parenchyma,^[95] CED was successfully applied for nanoscale materials targeted to glioblastoma xenografted in experimental animals, such as ¹²⁵I-labeled EGF incorporating and heavily boronated compounds linked

to a dendrimer scaffold for BNCT,^[96] non-PEGylated liposomes loaded with MRI-enhancement and chemotherapy agents,^[97] lipid “nanocapsules” labeled with a fluorescent marker and loaded with the drug paclitaxel,^[98] multifunctional dendriworms bearing siRNA cargo,^[87] and MRI-contrast enhancing magnetic nanoparticles.^[99]

Although there are obstacles in application of PDT in CNS, abovementioned obligatory surgical procedure allows applying of light-based techniques for intraoperative (application of light to a surgery cavity) or postoperative (via implanted optical fiber) adjuvant therapy. Progress in modern optical fiber technology enables successful photo-stimulation for precise dissection and selective control of disease circuitries in the CNS applicable, for example, to the treatment of Parkinsonism and major depression.^[100]

Employing of magnetic functionalities convey great advantage because the magnetic field can penetrate natural barriers such as skin, tissues and bones, and the application of an external magnetic stimulus is technically straightforward. For example, MRI employs a static field supplied by clinical hardware, while high frequency *ac* magnetic fields provided by an electromagnet or coil are used for cancer thermal therapies. A novel approach utilizing low *ac* field magnitudes for magneto-mechanical cancer destruction^[4] does not require heavy electromagnets and costly energy consumption, yet remains to be tested *in vivo*.

7. Conclusions and Outlook

The molecular design of novel materials at the nanoscale is a cutting-edge research area with great expectations to contribute greatly to every sphere of life in the near future. In addition to emergent challenges connected with growing societal demands for clean energy and global economic prosperity improvements to the quality of life require upgraded medical technologies to combat life-threatening diseases. The treatment of brain cancer remains one of the most challenging areas in oncology. Two hallmark capacities of nanoengineered materials—targeted specific delivery to the tumor, and synergistic assembly of multifunctional entities in hybrid structures—may lead to innovative diagnostics, intra- and post-surgical imaging and postoperative therapies, and great improvements to patient survival rates. Multidisciplinary approaches utilizing input from materials science, the life sciences, molecular medicine, and nanotechnology will result in revolutionary breakthroughs in the field. Despite the vibrant expansion of innovative nanoplateforms, from the design of smart functional materials, to their translation to medical research, the path from bench-to-bedside remains extensive and long. The majority of the nanotechnology approaches applied in brain oncology reported in this article are in the stages of *in vitro* or animal model testing. Prior to the use of nanoengineered materials in clinical applications, major concerns, including biocompatibility and biodistribution, biosafety, side-effects, and long-term effects have to be addressed. Furthermore, personalized diagnostics and the identification of unique biological targets (epitope sequences), related to problems posed by disease variance, appear to be essential for clinical success. In coming years, we may expect growing numbers

of reports involving novel hybrid structures based upon nucleic acids, such as siRNAs for the targeted silencing of the major genetic pathways associated with brain cancer development and progression, and single strand DNA short aptamers for efficient, inexpensive, and non-immunogenic alternatives to antibodies. Finally, an application of nanoscale hybrid materials in combination with advanced engineered implantable devices (e.g. CED, optical fibers, wafers) may radically improve therapeutic results and remarkably shorten the bench-to bedside transition. Tremendous interdisciplinary efforts are expected to bring contemporary medical technologies in brain cancer treatment to unprecedented new levels.

Acknowledgements

I am grateful to all of my collaborators and colleagues for their enthusiasm and contribution to our inspiring multidisciplinary alliance. I would like to acknowledge Dr. I. Ulasov and Prof. M. S. Lesniak from University of Chicago, Dr. V. Novosad, Dr. D.-H. Kim, Dr. S. Bader, Dr. B. Lai and Dr. N. M. Dimitrijevic of Argonne National Laboratory. Special appreciation to Dr. T. Rajh for introducing me to the field of semiconductor nanoparticles. I thank Dr. A. Datesman and Dr. V. Novosad for critical and thoughtful reading of this manuscript. The work at the Center for Nanoscale Materials at Argonne National Laboratory was supported by UChicago Argonne, LLC, Operator of Argonne National Laboratory (ANL). ANL, a U.S. Department of Energy Office of Science laboratory, is operated under Contract No. DE-AC02-06CH11357.

Received: December 24, 2010

Revised: February 28, 2011

Published online:

- [1] <http://grants1.nih.gov/grants/guide/rfa-files/RFA-CA-09-012.html>
- [2] N. A. Kotov, J. O. Winter, I. P. Clements, E. Jan, B. P. Timko, S. Campidelli, S. Pathak, A. Mazzatenta, C. M. Lieber, M. Prato, R. V. Bellamkonda, G. A. Silva, N. W. S. Kam, F. Patolsky, L. Ballerini, *Adv. Mater.* **2009**, *21*, 3970.
- [3] a) A. Jordan, R. Scholz, K. Maier-Hauff, F. K.H. van Landeghem, N. Waldoefner, U. Teichgraber, J. Pinkernelle, H. Bruhn, F. Neumann, B. Thiesen, A. von Deimling, R. Felix, *J. Neurooncol.* **2006**, *78*, 7; b) K. Maier-Hauff, R. Rothe, R. Scholz, U. Gneveckow, P. Wust, B. Thiesen, A. Feussner, A. von Deimling, N. Waldoefner, R. Felix, A. Jordan, *J. Neurooncol.* **2007**, *81*, 53; c) B. Thiesen, A. Jordan, *Int. J. Hyperthermia* **2008**, *24*, 467; d) F. K. H. van Landeghem, K. Maier-Hauff, A. Jordan, K.-T. Hoffmann, U. Gneveckow, R. Scholz, B. Thiesen, W. Bruck, A. von Deimling, *Biomaterials* **2009**, *30*, 52.
- [4] D.-H. Kim, E. A. Rozhkova, I. V. Ulasov, S. D. Bader, T. Rajh, M. S. Lesniak, V. Novosad, *Nat. Mater.* **2010**, *9*, 165.
- [5] E. A. Rozhkova, V. Novosad, D.-H. Kim, Pearson J., Divan, R., Rajh, T., Bader, S. D., *J. Appl. Phys.* **2009**, *105*, 07B306.
- [6] a) W. Kaim, N. S. Hosmane, *J. Chem. Sci.* **2010**, *122*, 7; b) I. B. Sivaev, V. V. Bregadze, *Eur. J. Inorg. Chem.* **2009**, 1433; c) J. D. Brockman, D. W. Nigg, M. F. Hawthorne, M. W. Lee, C. McKibben, *J. Radioanal. Nucl. Chem.* **2009**, *282*, 157.
- [7] W. H. Sweet, *N. Engl. J. Med.* **1951**, *245*, 875.
- [8] G.L. Locher, *Am. J. Roentgenol. Radium Ther.* **1936**, *36*, 1.
- [9] J. T. Huse, E. C. Holland, *Nat. Rev. Cancer* **2010**, *10*, 319.
- [10] D. N. Louis, H. Ohgaki, O. D. Wiestler, W. K. Cavenee, P. C. Burger, A. Jouvret, B. W. Scheithauer, P. Kleihues, *Acta Neuropathol.* **2007**, *114*, 97.
- [11] R. Stupp, W. P. Mason, M. J. van den Bent, M. Weller, B. Fisher, M. J.B. Taphoorn, K. Belanger, A. A. Brandes, C. Marosi, U. Bogdahn, J. Curschmann, R. C. Janzer, S. K. Ludwin, T. Gorlia, A. Allgeier, D. Lacombe, J. G. Cairncross, E. Eisenhauer, R. O. Mirimanoff, *N. Engl. J. Med.* **2005**, *352*, 987.
- [12] P. Y. Wen, S. Kesari, *N. Engl. J. Med.* **2008**, *359*, 492.
- [13] L. E. Gaspar, B. J. Fisher, D. R. Macdonald, D. V. LeBer, E. C. Halperin, S. C. Schold, J. G. Cairncross, *Int. J. Radiat. Oncol. Biol. Phys.* **1992**, *24*, 55.
- [14] R. J. Gilbertson, *Lancet Oncol.* **2004**, *5*, 209.
- [15] a) W. Debinski, D. M. Gibo, *Mol. Med.* **2000**, *6*, 440; b) A. Mintz, D. M. Gibo, B. Slagle-Webb, N. D. Christensen, W. Debinski, *Neoplasia* **2002**, *4*, 388; c) K. Kawakami, J. Taguchi, T. Murata, R. K. Puri, *Blood* **2001**, *97*, 2673; d) K. Kawakami, F. Takeshita, R. K. Puri, *J. Biol. Chem.* **2001**, *276*, 25114.
- [16] a) W. Debinski, D. Gibo, S. Hulet, J. Connor, G. Gillespie, *Cancer Res.* **1999**, *59*, 985; b) K. Kawakami, M. Kawakami, P. J. Snoy, S. R. Husain, R. K. Puri, *J. Exp. Med.* **2001**, *194*, 1743; c) J. Wykosky, D. M. Gibo, C. Stanton, W. Debinski, *Clin. Cancer Res.* **2008**, *14*, 199.
- [17] G. Zhou, G. J. Yet, W. Debinski, B. Roizman, *Proc. Natl. Acad. Sci. USA* **2002**, *99*, 15124.
- [18] R. J. Bernardi, A. R. Lowery, P. A. Thompson, S. M. Blaney, J. L. West, *J. Neurooncol.* **2008**, *86*, 165.
- [19] E. A. Rozhkova, I. Ulasov, B. Lai, N. M. Dimitrijevic, M. S. Lesniak, T. Rajh, *Nano Lett.* **2009**, *9*, 3337.
- [20] J. P. Celli, B. Q. Spring, I. Rizvi, C. L. Evans, K. S. Samkoe, S. Verma, B. W. Pogue, T. Hasan, *Chem. Rev.* **2010**, *110*, 2795.
- [21] a) E. Angell-Petersen, S. Spetalen, S. J. Madsen, C. H. Sun, Q. Peng, S. W. Carper, M. Sioud, H. Hirschberg, *J. Neurosurg. Toxicol. Oncol.* **2006**, *25*, 453; c) S. J. Madsen, E. Angell-Petersen, S. Spetalen, S. W. Carper, S. A. Ziegler, H. Hirschberg, *Lasers Surg. Med.* **2006**, *38*, 540; d) S. J. Madsen, C. H. Sun, B. J. Tromberg, V. P. Wallace, H. Hirschberg, *Photochem Photobiol.* **2000**, *72*, 128; e) P. J. Muller, B. C. Wilson, *Photochem. Photobiol.* **1987**, *46*, 929.
- [22] V. Simon, C. Devaux, A. Darmon, T. Donnet, E. Thienot, M. Germain, J. Honnorat, A. Duval, A. Pottier, E. Borghi, L. Levy, J. Marill, *Photochem. Photobiol.* **2010**, *86*, 213.
- [23] G. R. Reddy, M. S. Bhojani, P. McConville, J. Moody, B. A. Moffat, D. E. Hall, G. Kim, Y.-E. L. Koo, M. J. Woolliscroft, J. V. Sugai, T. D. Johnson, M. A. Philbert, R. Kopelman, A. Rehemtulla, B. D. Ross, *Clin. Cancer Res.* **2006**, *12*, 6677.
- [24] T. Rajh, N. M. Dimitrijevic, E. A. Rozhkova, in *Biomedical Nanotechnology* Vol. 726, (Ed. S. J. Hurst) Springer, Methods in Molecular Biology, **2011**.
- [25] a) T. Rajh, L. X. Chen, K. Lukas, T. Liu, M. C. Thurnauer, D. M. Tiede, *J. Phys. Chem. B* **2002**, *106*, 10543; b) T. Rajh, Z. Saponjic, J. Liu, N. M. Dimitrijevic, N. F. Scherer, M. Vega-Arroyo, P. Zapol, L. A. Curtiss, M. C. Thurnauer, *Nano Lett.* **2004**, *4*, 1017; c) N. M. Dimitrijevic, Z. Saponjic, B. M. Rabatic, T. Rajh, *J. Am. Chem. Soc.* **2005**, *127*, 1344.
- [26] N. M. Dimitrijevic, E. A. Rozhkova, T. Rajh, *J. Am. Chem. Soc.* **2009**, *131*, 2893.
- [27] S. Yamaguchi, H. Kobayashi, T. Narita, K. Kanehira, S. Sonezaki, Y. Kubota, S. Terasaka, Y. Iwasaki, *Photochem. Photobiol.* **2010**, *86*, 964.
- [28] a) A. Fujishima, X. Zhang, D. A. Tryk, *Surf. Sci. Rep.* **2008**, *63*, 515; b) K. Szaciowski, W. Macyk, A. Drzewiecka-Matuszek, M. Brindell, G. Stochel, *Chem. Rev.* **2005**, *105*, 2647; c) K. Sunada, T. Watanabe, K. Hashimoto, *J. Photochem. Photobiol. A: Chem.* **2003**, *156*, 227; d) M. Sokmen, F. Candan, Z. Sumer, *J. Photochem. Photobiol. A: Chem.* **2001**, *143*, 241; e) J. Theron, J. A. Walker, T. E. Cloete, *Crit. Rev. Microbiol.* **2008**, *34*, 43; f) P. Amezaga-Madrid, G. V. Nevarez-Moorillon, E. Orrantia-Borunda, M. Miki-Yoshida, *FEMS Microbiol. Lett.* **2002**, *211*, 183; g) R. R. Shah, S. Kaewgun, B. I. Lee, T.-R. J. Tzeng, *J. Biomed. Nanotechnol.* **2008**, *3*, 339; h) C. A. Linkous, G. J. Carter,

- D. B. Locuson, A. J. Ouellette, D. K. Slattery, L. A. Smitha, *Environ. Sci. Technol.* **2000**, *34*, 4754; i) K. Yamaguchi, T. Sugiyama, S. Kato, Y. Kondo, N. Ageyama, M. Kanekiyo, M. Iwata, Y. Koyanagi, N. Yamamoto, M. Honda, *J. Med. Virol.* **2008**, *80*, 1322.
- [29] a) R. Cai, K. Hashimoto, K. Itoh, Y. Kubota, A. Fujishima, *Bull. Chem. Soc. Jpn.* **1991**, *64*, 1268; b) R. X. Cai, Y. Kubota, T. Shuin, H. Sakai, K. Hashimoto, A. Fujishima, *Cancer Res.* **1992**, *52*, 2346; c) H. Sakai, E. Ito, R. X. Cai Yoshioka, Y. Kubota, K. Hashimoto, A. Fujishima, *Biochim. Biophys. Acta* **1994**, *1201*, 259; d) Y. Kubota, T. Shuin, C. Kawasaki, M. Hosaka, H. Kitamura, R. Cai, H. Sakai, K. Hashimoto, A. Fujishima, *Br. J. Cancer* **1994**, *70*, 1107; e) H. Sakai, R. Baba, K. Hashimoto, Y. Kubota, A. Fujishima, *Chem. Lett.* **1995**, *3*, 185; f) P.-J. Lu, I.-C. Ho, T.-C. Lee, *Mutat. Res., Genet. Toxicol. Environ. Mutagen.* **1998**, *414*, 15; g) T. Uchino, H. Tokunaga, M. Ando, H. Utsumi, *Toxicol. in Vitro* **2002**, *16*, 629; h) J. W. Seo, H. Chung, M. Y. Kim, J. Lee, I. H. Choi, J. Cheon, *Small* **2007**, *3*, 850; i) X. Juan, S. Yi, H. Junjie, C. Chunmei, L. Guoyuan, J. Yan, Z. Yaomin, J. Zhiyu, *Bioelectrochemistry* **2007**, *71*, 217; j) M. Kalbacova, J. M. Macak, F. Schmidt-Stein, C. T. Mierke, P. Schmuki, *Phys. Status Solidi RRL: Rapid Res. Lett.* **2008**, *2*, 194.
- [30] L. de la Garza, Z. V. Saponjic, N. M. Dimitrijevic, M. C. Thurnauer, T. Rajh, *J. Phys. Chem. B* **2006**, *110*, 680.
- [31] a) T. Lopez, S. Recillas, P. Guevara, J. Sotelo, M. Alvarez, J. A. Odriozola, *Acta Biomaterialia* **2008**, *4*, 2037; b) T. Lopez, F. Figueras, J. Manjarrez, J. Bustos, M. Alvarez, J. Silvestre-Albero, F. Rodriguez-Reinoso, A. Martinez-Ferre, E. Martinez, *Eur. J. Med. Chem.* **2010**, *45*, 1982; c) T. Lopez, T. E. Ortiz, P. Quintana, R. D. Gonzalez, *Coll. Surf. A* **2007**, *300*, 3.
- [32] P. K. Jain, K. S. Lee, I. H. El-Sayed, M. A. El-Sayed, *J. Phys. Chem. B* **2006**, *110*, 7238.
- [33] P. K. Jain, X. Huang, I. H. El-Sayed, M. A. El-Sayed, *Acc. Chem. Res.* **2008**, *41*, 1578.
- [34] J. Chen, M. Yang, Q. Zhang, E. C. Cho, C. M. Cobley, C. Kim, C. Claus, L. V. Wang, M. J. Welch, Y. Xia, *Adv. Funct. Mater.* **2010**, *20*, 3684.
- [35] L. R. Hirsch, A. M. Gobin, A. R. Lowery, F. Tam, R. A. Drezek, N. J. Halas, J. L. West, *Ann. Biomed. Eng.* **2006**, *34*, 15.
- [36] A. M. Gobin, M. H. Lee, N. J. Halas, W. D. James, R. A. Drezek, J. L. West, *Nano Lett.* **2007**, *7*, 1929.
- [37] S. Wang, K.-J. Chen, T.-H. Wu, H. Wang, W.-Y. Lin, M. Ohashi, P.-Y. Chiou, H.-R. Tseng, *Angew. Chem. Int. Ed.* **2010**, *49*, 3777.
- [38] X. Huang, I. H. El-Sayed, W. Qian, M. A. El-Sayed, *J. Am. Chem. Soc.* **2006**, *128*, 2115.
- [39] X. Wang, Y. Pang, G. Ku, X. Xie, G. Stoica, L. V. Wang, *Nat. Biotechnol.* **2003**, *21*, 803.
- [40] M. Xu, L. V. Wang, *Rev. Sci. Instrum.* **2006**, *77*, 041101.
- [41] D. Pan, M. Pramanik, A. Senpan, J. S. Allen, H. Zhang, S. A. Wickline, L. V. Wang, G. M. Lanza, *FASEB Journal* **2011**, *25*, 1.
- [42] M.-L. Li, J.-T. Oh, X. Xie, G. Ku, W. Wang, C. Li, G. Lungu, G. Stoica, L. V. Wang, *Proceedings of the IEEE* **2008**, *96*, 481.
- [43] Y. Wang, X. Xie, X. Wang, G. Ku, K. L. Gill, D. P. O'Neal, G. Stoica, L. V. Wang, *Nano Lett.* **2004**, *4*, 1689.
- [44] X. Yang, S. E. Skrabalak, Z.-Y. Li, Y. Xia, L. V. Wang, *Nano Lett.* **2007**, *7*, 3798.
- [45] W. Lu, Q. Huang, G. Ku, X. Wen, M. Zhou, D. Guzato, P. Brecht, R. Su, A. Oraevsky, L. V. Wang, C. Li, *Biomaterials* **2010**, *31*, 2617.
- [46] R. Popovtzer, A. Agrawal, N. A. Kotov, A. Popovtzer, J. Balter, T. E. Carey, R. Kopelman, *Nano Lett.* **2008**, *8*, 4593.
- [47] O. T. Bruns, H. Ittrich, K. Peldschus, M. G. Kaul, U. I. Tromsdorf, J. Lauterwasser, M. S. Nikolic, B. Mollwitz, M. Merkel, N. C. Bigall, S. Sapra, R. Reimer, H. Hohenberg, H. Weller, A. Eychmüller, G. Adam, U. Beisiegel, J. Heeren, *Nat. Nanotechnol.* **2009**, *4*, 193.
- [48] M. Ferrari, *Nature Rev. Cancer* **2005**, *5*, 16138.
- [49] R. Hergt, S. Dutz, R. Muller, M. Zeisberger, *J. Phys. Condens. Matter.* **2006**, *18*, S2919.
- [50] K. M. Krishnan, *IEEE Trans. Mag.* **2010**, *46*, 2523.
- [51] Q. A. Pankhurst, N. K. Thanh, S. K. Jones, J. Dobson, *J. Phys D: Appl. Phys.* **2009**, *42*, 224001.
- [52] C. C. Berry, *J. Phys. D: Appl. Phys.* **2009**, *42*, 224003.
- [53] A. G. Roca, R. Costo, A. F. Rebolledo, S. Veintemillas-Verdaguer, P. Tartaj, T. Gonzalez-Carreno, M. P. Morales, C. J. Serna, *J. Phys. D: Appl. Phys.* **2009**, *42*, 224002.
- [54] R. Hao, R. Xing, Z. Xu, Y. Hou, S. Gao, S. Sun, *Adv. Mater.* **2010**, *22*, 2729.
- [55] J. Dobson, *Nat. Nanotechnol.* **2008**, *3*, 139.
- [56] R. J. Mannix, S. Kumar, F. Cassiola, M. Montoya-Zavala, E. Feinstein, M. Prentiss, D. E. Ingber, *Nature Nanotechnology* **2007**, *3*, 36.
- [57] R. K. Gilchrist, R. Medal, W. D. Shorey, R. C. Hanselman, J. C. Parrott, C. B. Taylor, *Ann. Surg.* **1957**, *146*, 596.
- [58] R. Qiao, C. Yang, M. Gao, *J. Mater. Chem.* **2009**, *19*, 6274.
- [59] C. F. Galdes, S. Laurent, *Contrast Media Mol. Imag.* **2009**, *4*, 1.
- [60] W. S. Enochs, G. Harsh, F. Hochberg, R. Weissleder, *J. Magn. Reson. Imaging* **1999**, *9*, 228.
- [61] E. A. Neuwelt, P. Varallyay, A. G. Bago, L. L. Muldoon, G. Nesbit, R. Nixon, *Neuropathol. Appl. Neurobiol.* **2004**, *30*, 456.
- [62] P. Varallyay, G. Nesbit, L. L. Muldoon, R. R. Nixon, J. Delashaw, J. I. Cohen, A. Petrillo, D. Rink, E. A. Neuwelt, *Am. J. Neuroradiol.* **2002**, *23*, 510.
- [63] a) O. Veisheh, C. Sun, J. Gunn, N. Kohler, P. Gabikian, D. Lee, N. Bhattarai, R. Ellenbogen, R. Sze, A. Hallahan, J. Olson, M. Zhang, *Nano Lett.* **2005**, *5*, 1003; b) C. Sun, O. Veisheh, J. Gunn, C. Fang, S. Hansen, D. Lee, R. Sze, R. G. Ellenbogen, J. Olson, M. Zhang, *Small* **2008**, *4*, 372; c) M. Veisheh, P. Gabikian, S. B. Bahrami, O. Veisheh, M. Zhang, R. C. Hackman, A. C. Ravanpay, M. R. Stroud, Y. Kusuma, S. J. Hansen, D. Kwok, N. M. Munoz, R. W. Sze, W. M. Grady, N. M. Greenberg, R. G. Ellenbogen, J. M. Olson, *Cancer Res.* **2007**, *67*, 6882.
- [64] M. Kumar, Z. Medarova, P. Pantazopoulos, G. Dai, A. Moore, *Magnetic Resonance in Medicine* **2010**, *63*, 617.
- [65] K. Chen, J. Xie, H. Xu, D. Behera, M. H. Michalski, S. Biswal, A. Wang, X. Chen, *Biomaterials* **2009**, *30*, 6912.
- [66] S. X. Wang, G. Li, *IEEE Trans. Mag.* **2008**, *44*, 1687.
- [67] A. Fu, W. Hu, L. Xu, R. J. Wilson, H. Yu, S. J. Osterfeld, S. S. Gambhir, S. X. Wang, *Angew. Chem. Int. Ed.* **2009**, *48*, 1620.
- [68] G. Zabow, S. Dodd, J. Moreland, A. Koretsky, *Nature* **2008**, *453*, 1058.
- [69] G. Zabow, S. J. Dodd, J. Moreland, A. P. Koretsky, *Nanotechnology* **2009**, *20*, 385301.
- [70] L. Mair, K. Ford, R. Alam, R. Kole, M. Fisher, R. Superfine, *J. Biomed. Nanotechnol.* **2009**, *5*, 182.
- [71] D.-H. Kim, P. Karavayev, E. A. Rozhkova, J. Pearson, V. Yefremenko, S. D. Bader, V. Novosad, *J. Mater. Chem.* **2011**, DOI: 10.1039/c1jm10272a.
- [72] I. L. Medintz, H. T. Uyeda, E. R. Goldman, H. Mattoussi, *Nature Materials* **2005**, *4*, 435.
- [73] C. C. Lee, J. A. MacKay, J. M. Frechet, F. C. Szoka, *Nature Biotechnology* **2005**, *23*, 1517.
- [74] J. Wan, X. Meng, E. Liu, K. Chen, *Nanotechnology* **2010**, *21*, 235104.
- [75] a) C. Tuerk, L. Gold, *Science* **1990**, *249*, 505; b) D. H. J. Bunka, P. G. Stockley, *Nature* **2006**, *4*, 588.
- [76] L. Cerchia, C. L. Esposito, A. H. Jacobs, B. Tavitian, V. de Franciscis, *PLoS ONE* **2009**, *4*, e7971.
- [77] D. W. Hwang, H. Y. Ko, J. H. Lee, H. Kang, S. H. Ryu, I. C. Song, D. S. Lee, S. Kim, *J. Nuclear Med.* **2010**, *51*, 98.
- [78] A. M. Derfus, W. C. W. Chan, S. N. Bhatia, *Nano Lett.* **2004**, *4*, 11.
- [79] S. Deka, A. Quarta, M. G. Lupo, A. Falqui, S. Boninelli, C. Giannini, G. Morello, M. De Giorgi, G. Lanzani, C. Spinella, R. Cingolani,

- Teresa Pellegrino, L. Manna, *J. Am. Chem. Soc.* **2009**, *131*, 2948.
- [80] X.-C. Chen, Y.-L. Deng, Y. Lin, D.-W. Pang, H. Qing, F. Qu, H.-Y. Xie, *Nanotechnology* **2008**, *19*, 235105.
- [81] Z. Li, P. Huang, R. He, J. Lin, S. Yang, X. Zhang, Q. Ren, D. Cui, *Mater. Lett.* **2010**, *64*, 375.
- [82] a) S. J. Clarke, C. A. Hollmann, Z. Zhang, D. Suffern, S. E. Bradforth, N. M. Dimitrijevic, W. G. Minarik, J. L. Nadeau, *Nat. Mater.* **2006**, *5*, 409; b) D. R. Cooper, N. M. Dimitrijevic, J. L. Nadeau, *Nanoscale* **2010**, *2*, 114.
- [83] A. Fire, S. Xu, M. K. Montgomery, S. A. Kostas, S. E. Driver, C. C. Mello, *Nature* **1998**, *391*, 806.
- [84] J. Jung, A. Solanki, K. A. Memoli, K.-ichiro Kamei, H. Kim, M. A. Drahl, L. J. Williams, H.-R. Tseng, K. B. Lee, *Angew. Chem. Int. Ed.* **2010**, *49*, 103.
- [85] a) A. J. Ekstrand, N. Sugawa, C. D. James, V. P. Collins, *Proc. Natl. Acad. Sci. USA* **1992**, *89*, 4309; b) P. A. Humphrey, A. J. Wong, B. Vogelstein, M. R. Zalutsky, G. N. Fuller, G. E. Archer, H. S. Friedman, M. M. Kwatra, S. H. Bigner, D. D. Bigner, *Proc. Natl. Acad. Sci. USA* **1990**, *87*, 4207.
- [86] Q. W. Fan, W. A. Weiss, *Oncogene* **2005**, *24*, 829; a) I. Vivanco, C. L. Sawyers, *Nature Rev. Cancer* **2002**, *2*, 489; b) F. Yamoutpour, V. Bodernpudi, S. E. Park, W. H. Pan, M. J. Mauzy, R. A. Kratzke, A. Dudek, D. A. Potter, R. A. Woo, D. M. O. Rourke, D. J. Tindall, F. Farassati, *Mol. Cancer Ther.* **2008**, *7*, 3586.
- [87] A. Agrawal, D.-H. Min, N. Singh, H. Zhu, A. Birjiniuk, G. von Maltzahn, T. J. Harris, D. Xing, S. D. Woolfenden, P. A. Sharp, A. Charest, S. Bhatia, *ACS Nano* **2009**, *3*, 2495.
- [88] a) G. A. Silva, *Surgical Neurology* **2007**, *67*, 113; b) S. M. Hussain, L. K. Braydich-Stolle, A. M. Schrand, R. C. Murdock, K. O. Yu, D. M. Mattie, J. J. Schlager, M. Terrones, *Adv. Mater.* **2009**, *21*, 1549; c) W. H. Suha, Y.-H. Suhb, G. D. Stucky, *Nano Today* **2009**, *4*, 27; d) Z. Yang, Z. W. Liu, R. P. Allaker, P. Reip, J. Oxford, Z. Ahmad, G. Ren, *J. R. Soc. Interface* **2010**, *7*, S411; e) H. Sarin, A. S. Kanevsky, H. Wu, K. R. Brimacombe, S. H. Fung, A. A. Sousa, S. Auh, C. M. Wilson, K. Sharma, M. A. Aronova, R. D. Leapman, G. L. Griffiths, M. D. Hall, *J. Trans. Med.* **2008**, *6*, 80; f) H. Sarin, A. S. Kanevsky, H. Wu, A. A. Sousa, C. M. Wilson, M. A. Aronova, G. L. Griffiths, R. D. Leapman, H. Q. Vo, *J. Trans. Med.* **2009**, *7*, 51.
- [89] N. J. Abbott, L. Ronnback, E. Hansson, *Nature Rev. Neurosci.* **2006**, *7*, 41.
- [90] a) R. K. Jain, *Cancer Metastasis Rev.* **1987**, *6*, 559; b) H. F. Dvorak, J. A. Nagy, D. Feng, L. F. Brown, A. M. Dvorak, *Curr. Top. Microbiol. Immunol.* **1999**, *237*, 97.
- [91] S. K. Hobbs, W. L. Monsky, F. Yuan, W. G. Roberts, L. Griffith, V. P. Torchilin, R. K. Jain, *Proc. Natl. Acad. Sci. USA* **1998**, *95*, 4607.
- [92] a) W. Sun, C. Xie, H. Wang, Y. Hu, *Biomaterials* **2004**, *25*, 3065; b) W. Sun, H. Wang, C. Xie, Y. Hu, X. Yang, H. Xu, *J. Controlled Release* **2006**, *115*, 259.
- [93] a) H. Maeda, J. Greish, K. Fang, *Adv. Polymer Sci.* **2006**, *193*, 103; b) W. M. Partridge, *Pharm. Res.* **2007**, *24*, 1733; c) N. T. Huynh, C. Passirani, P. Saulnier, J. P. Benoit, *Int. J. Pharmaceutics* **2009**, *379*, 201.
- [94] H. Sarin, *J. Translational Med.* **2009**, *7*, 77.
- [95] R. H. Bobo, D. W. Laske, A. Akbasak, P. F. Morrison, R. L. Dedrick, E. H. Oldfield, *Proc. Natl. Acad. Sci. USA* **1994**, *91*, 2076.
- [96] W. Yang, R. F. Barth, D. M. Adams, Michael J. Ciesielski, R. A. Fenstermaker, S. Shukla, W. Tjarks, M. A. Caligiuri, *Cancer Res.* **2002**, *62*, 6552.
- [97] A. Y. Grahn, K. S. Bankiewicz, M. Dugich-Djordjevic, J. R. Bringas, P. Hadaczek, G. A. Johnson, S. Eastman, M. Luz, *J. Neurooncol.* **2009**, *95*, 185.
- [98] S. Vinchon-Petit, D. Jarnet, A. Paillard, J.-P. Benoit, E. Garcion, P. Menei, *J. Neurooncol.* **2010**, *97*, 195.
- [99] a) B. Perlstein, Z. Ram, D. Daniels, A. Ocherashvili, Y. Roth, S. Margel, Y. Mardor, *Neuro Oncol.* **2008**, *10*, 153; b) C. G. Hadjipanayis, R. Machaidze, M. Kaluzova, L. Y. Wang, A. J. Schuette, H. W. Chen, X. Y. Wu, H. Mao, *Cancer Res.* **2010**, *70*, 6303.
- [100] V. Gradinaru, M. Mogri, K. R. Thompson, J. M. Henderson, K. Deisseroth, *Science* **2009**, *324*, 354.